Journal of Materials Chemistry C

Materials for optical and electronic devices

www.rsc.org/MaterialsC

Volume 1 | Number 24 | 28 June 2013 | Pages 3749–3888

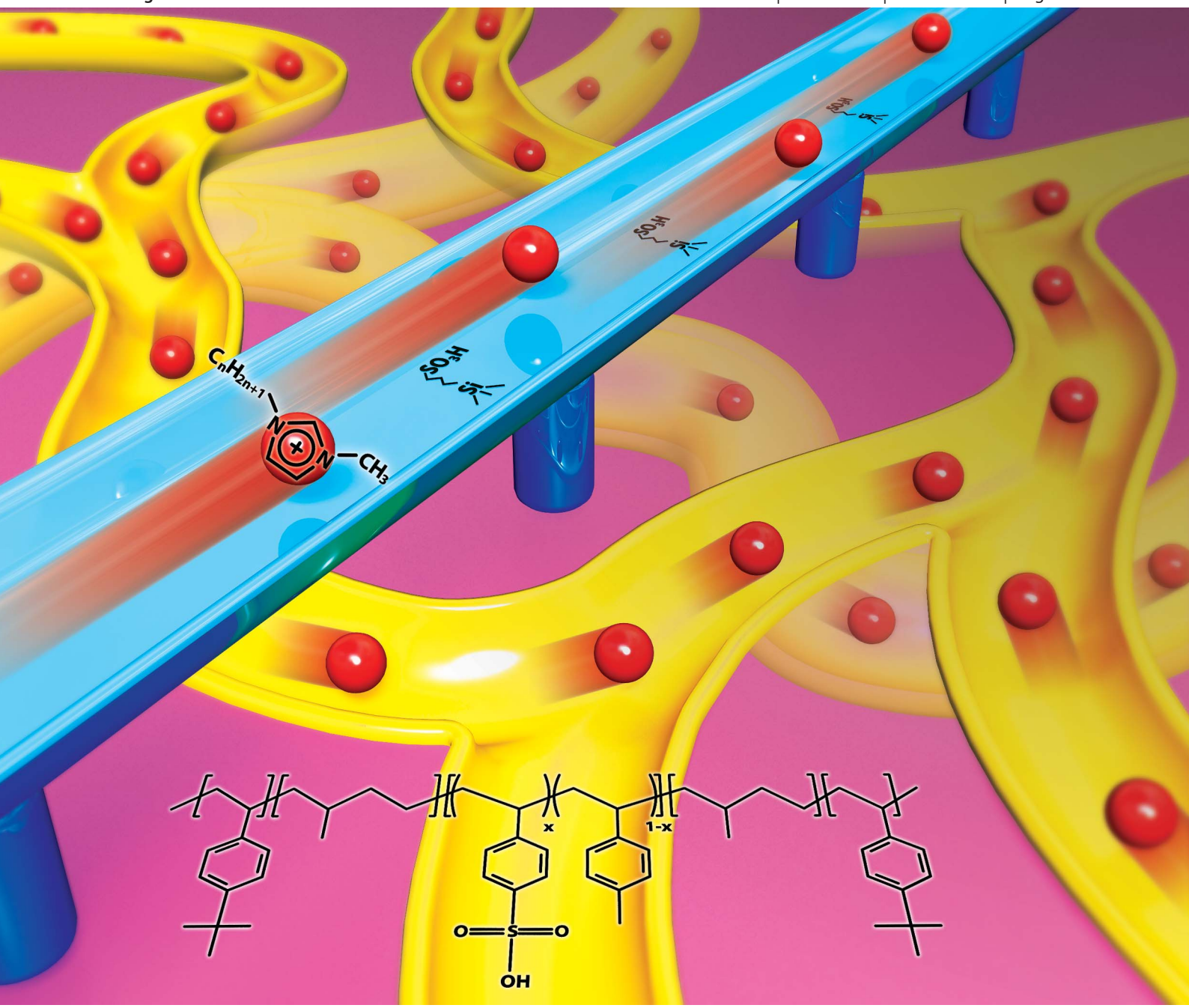

ISSN 2050-7526

RSC Publishing

PAPER

Chong Min Koo *et al.*

High-strain air-working soft transducers produced from nanostructured block copolymer ionomer/silicate/ionic liquid nanocomposite membranes

Journal of Materials Chemistry C

RSC Publishing

PAPER

View Article Online
View Journal | View Issue

Cite this: J. Mater. Chem. C, 2013, 1, 3784

High-strain air-working soft transducers produced from nanostructured block copolymer ionomer/silicate/ionic liquid nanocomposite membranes†

Jang-Woo Lee,‡[a] Seunggun Yu,[a] Soon Man Hong[a] and Chong Min Koo*[ab]

The present work demonstrates that nanostructured middle-block sulfonated styrenic pentablock copolymer ionomer (SSPB)/sulfonated montmorillonite (s-MMT) nanocomposite membranes, incorporating bulky imidazolium ionic liquid (IL), act as novel polymer electrolytes for air-working ionic polymer–metal composite (IPMC) actuators. The microphase-separated big-size ionic domains of the SSPB on the scale of several tens of nanometers and the role of s-MMT as an ionic bridge between the ion channels resulted in not only unexpectedly larger ion conductivity, larger air-working bending displacement and faster bending rate, without conventional IPMC drawbacks, including back relaxation and a sacrifice of mechanical strength, but also higher energy efficiency actuation than Nafion. Interestingly, the bending displacement, bending rate, and charge-specific displacement of the nanocomposite IPMC increased with the increase in bulkiness of the ILs because of the strong ion pumping effect of the bulky immidazolium cations in the size-matched big ion channels of the nanocomposite membrane.

Received 5th March 2013
Accepted 9th April 2013

DOI: 10.1039/c3tc30414k

www.rsc.org/MaterialsC

Introduction

Ionic polymer–metal composite (IPMC) transducers, which facilitate the conversion of electrical energy to mechanical energy, have had a considerable amount of attention as potential candidates for nature-inspired polymer-based compact actuators, sensors, artificial muscles, and microrobots. The attraction has mainly been due to their large, fast, and soft bending actuation under fairly low operating voltages (1–5 V), which have not been realized by other electroactive materials, such as dielectric elastomers, ferroelectric polymers, and ceramic actuators.[1,2]

The IPMC transducers have a simple capacitor structure consisting of an ion-conducting polymer membrane incorporating mobile ions and inner solvent, and electrodes on both surfaces of the membrane. The electromechanical energy conversion for the IPMC actuator is typically harnessed from the displacement and force produced through a bending motion in cantilever configuration. The bending mechanism is referred to as the transport of mobile ions motivated by an external electric stimulus, followed by the electro-osmotic drag of a conduction-activating inner solvent, such as water. This ion/solvent migration induces an asymmetric volume change between both sides of IPMC; thus, generating the bending deformation of IPMC mostly to the positively charged anodic direction of the electrode.[3,4]

Nafion, developed by Walther Grot of DuPont in the late 1960s, has been the most commonly used synthetic polymer ionomer membrane for IPMC actuators. The ionic passages clustered with sulfonic acid groups in Nafion on the scale of a few nanometers produce high proton conductivity, and the tetrafluoroethylene backbone of the Nafion provides thermal, chemical, and mechanical stability.[5,6] Despite the advantages of Nafion, some fatal drawbacks including a fast back relaxation and an early dehydration were found in the IPMC devices.[6–11] In the back relaxation behavior, the bending direction turns back towards the initial position after reaching a maximum forward displacement during the continuous application of dc voltage. The back relaxation is caused by the diffusing back of water to the anode after full bending, and limits the frequency range and accuracy of the actuator's motion control.[8,9] The early loss of water out of the IPMC during actuation causes a reduction of ionic flux followed by a rapid decay of actuation performance in air operation. Thus, the working place of the hydrated Nafion is

[a]Center for Materials Architecturing, Institute for Multi-Disciplinary Convergence of Materials, Korea Institute of Science and Technology (KIST), Seoul 136-791, Republic of Korea. E-mail: koo@kist.re.kr; Fax: +82 2 958 5309; Tel: +82 2 958 6872
[b]Nanomaterials Science and Engineering, University of Science and Technology, Daejeon 305-350, Republic of Korea

† Electronic supplementary information (ESI) available: Characterization of s-MMT (detailed synthetic procedure, WAXD, thermogravimetry, and EDS), chemical structures of C2, C4, C6, and C8 ILs, SAXS profiles of SSPB/MMT/IL and SSPB/s-MMT/IL membranes with C2, C4, C6, and C8 ILs, and tip displacement *vs.* time curves and cyclic voltammograms of SSPB/MMT/IL and SSPB/s-MMT/IL IPMCs with C2, C4, C6, and C8 ILs. See DOI: 10.1039/c3tc30414k

‡ Present address: Department of Applied Chemistry, Graduate School of Engineering, Hiroshima University, Higashi-Hiroshima 739-8527, Japan. E-mail: jwlee@hiroshima-u.ac.jp

limited to underwater, despite many potential applications involving working in air.[6,7]

Many Nafion-based IPMCs incorporating organic solvents with high boiling temperatures or ionic liquids (ILs, ionic salts in the liquid state at room temperature), instead of water-incorporated ones, have been proposed. However, the performance of their air-working was much inferior to that of hydrated Nafion-based IPMC because water as an inner solvent typically produces the best dissociation ability of mobile ions, the smallest viscosity, and consequently the greatest proton conductivity in the Nafion membrane.[12–14]

Thus, a great deal of effort has been addressed to the development of new polymer ionomer membranes for the air-working IPMC to replace Nafion since the last decade.[6–11,15–17] The new polymers have included: sulfonated polystyrenes,[7] sulfonated poly(vinyl alcohol)s,[6] sulfonated poly(arylene ether sulfone)s,[8] sulfonated ethylene vinyl alcohol copolymers,[9] fluorinated acrylic copolymers,[15] fluoropolymers grafted with sulfonated polystyrene,[10] sulfonated poly(styrene-*alt*-maleimide)-incorporated poly(vinylidene fluoride) semi-interpenetrating polymer networks (semi-IPNs),[11] and many others.[16,17] Most of them, however, failed to offer the desired ionic conductivities and IPMC actuation performances beyond those of Nafion.

In recent years, a handful of nanostructured block copolymer ionomers, such as sulfonated poly(styrene-*b*-ethylene-*co*-butylene-*b*-styrene) (SSEBS) triblock copolymer and poly((*t*-butyl-styrene)-*b*-(ethylene-*r*-propylene)-*b*-(styrene-*r*-styrene sulfonate)-*b*-(ethylene-*r*-propylene)-*b*-(*t*-butyl-styrene)) (*t*BS-EP-SS-EP-*t*BS; SSPB) pentablock copolymer have been considered as alternatives to Nafion for IPMC applications. These nanostructured block copolymer ionomers have been expected to produce well defined microphase-separated ionic domains on the scale of several tens of nanometers, which could work as more effective ion conduction channels than very small ionic clusters of Nafion on the scale of a few nanometers. In addition, the size and microstructure of the ionic domains could be well controlled by tailoring the fraction of each block unit and molecular weight of the block polymer ionomers.[18–20] In 2007, Wang *et al.* proposed the SSEBS triblock copolymer ionomer consisting of partially sulfonated styrene end blocks imparting not only ion-conductive character but also mechanical strength, and an aliphatic middle block imparting mechanical flexibility and toughness.[18] The triblock structure of SSEBS resulted in coarse mechanical strength in the hydrated state and poor actuation performance, because hydration of the sulfonated styrene end blocks significantly sacrificed the mechanical strength of SSEBS. In 2011 and 2012, Vargantwar *et al.* reported the SSPB pentablock copolymer with a selectively sulfonated middle block as a new nanostructured polymer ionomer of IPMC.[19,20] Selective solvent incorporation into the sulfonated styrene (SS) middle blocks rarely sacrificed the mechanical strength of SSPB because the glassy hard *t*BS end blocks and the rubbery aliphatic EP inner blocks were still responsible for the mechanical strength and toughness, respectively. Thus, the SSPB IPMCs incorporating glycerol and ethylene glycol as inner solvents generated a considerable bending strain. At almost the same time in February, 2012, Lee *et al.* independently reported that the hydrated SSPB/sulfonated montmorillonite (s-MMT) nanocomposite-based IPMCs consisting of SSPB and s-MMT fillers revealed much larger bending displacements and blocking forces than SSPB, owing to strong interactions between mobile ions and sulfonated groups on the surface of s-MMT fillers.[21] Nonetheless, so far, the air-working property of nanostructured SSPB block copolymer ionomer/s-MMT nanocomposites has not been investigated.

Herein, we demonstrate that the nanostructured SSPB block copolymer ionomer/functionalized layered silicate nanocomposite membranes, incorporating bulky imidazolium ionic liquids (IL), work as novel air-working IPMC polymer electrolytes. The well-defined microphase-separated ionic domains of the nanostructured ionomers on the scale of several tens of nanometers and the impregnation of sulfonated silicate fillers into the nanostructured ionomers resulted in not only an unexpectedly larger air-working bending displacement and faster bending rate without the conventional IPMC drawbacks, including back relaxation and a sacrifice of mechanical strength, but also a larger energy efficient actuation performance than Nafion, as illustrated in Fig. 1a. Interestingly, the air-working IL-incorporated nanocomposite IPMC revealed a much larger bending displacement and faster bending rate than the hydrated nanocomposite IPMC. Moreover, the bending displacement, bending rate, and charge-specific displacement of the nanostructured ionomer/functionalized silicate nanocomposite IPMC increased with the increase in bulkiness of the ILs because of the strong pumping effect of the bulky immidazolium cations in the size-matched big ion channels of the nanostructured block copolymer ionomer/functionalized silicate nanocomposite membranes.

Results and discussion

Three types of membranes, including SSPB, SSPB/MMT, and SSPB/s-MMT, were fabricated *via* solution blending and investigated. The chemical structure and molecular information of the SSPB pentablock copolymer ionomer used in this study are shown in Fig. 1b and Table 1. The SSPB revealed a well-defined microphase-separated morphology in which the repeating domain spacing (d), composed of alternating styrene-rich regions (ionic phase) and aliphatic EP-rich regions (non-ionic phase), was *ca.* 30 nm, and the average diameter of the ionic channel regions was *ca.* 20 nm. Nafion however had narrow ion clusters of below 3.8 nm, as shown in Fig. 1e and g. Two types of layered silicates, pristine Na^+-MMT (MMT) and the sulfonated MMT (s-MMT) (Fig. 1c) were introduced to the SSPB block copolymer ionomer with a fixed filler content of 8 wt%. MMT had the ion exchange capacity of 0.91 meq. per 1 g silicate, which was attributed to the presence of $Si–O^-$ anions on the surface. On the other hand, s-MMT had sulfonic acid anions with the density of 0.33 mmol g^{-1} on the basis of thermogravimetric analysis[24] as listed in Table 1 (ESI, Fig. S1–S4,† for the detailed descriptions of both silicates including the synthetic procedure, the structural identification, and the quantitative/qualitative analyses). In Fig. 1h, the SSPB/s-MMT and

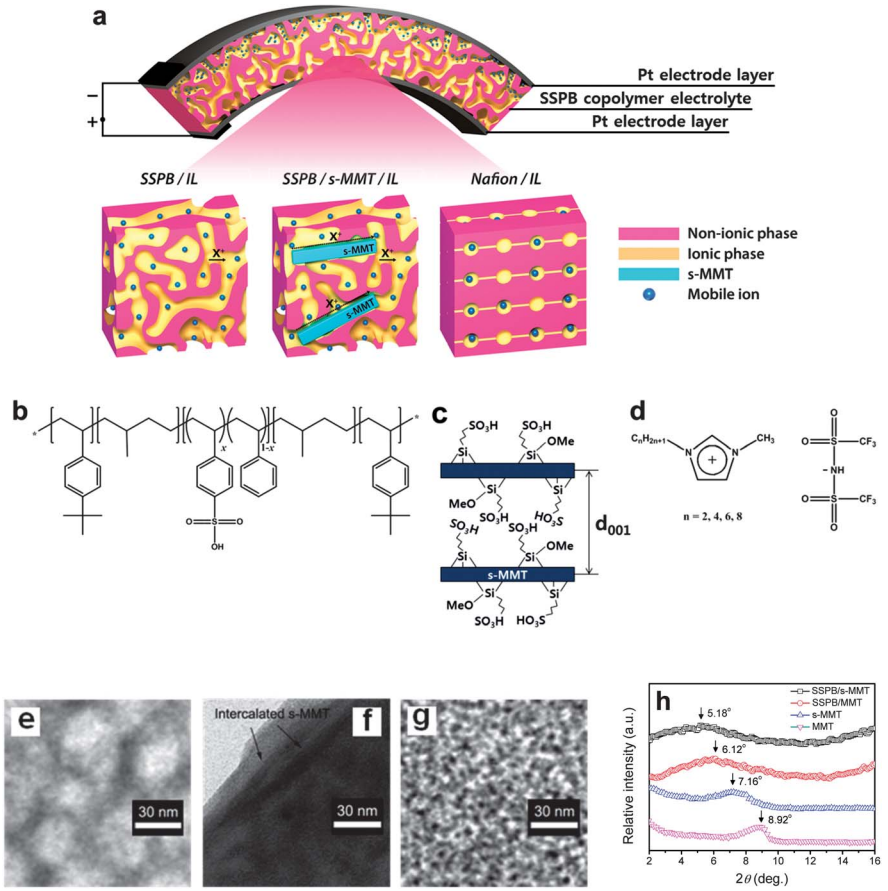

Fig. 1 (a) A schematic illustration of the IPMCs made of SSPB/IL, SSPB/s-MMT/IL and Nafion/IL membranes operating at dc potential. SSPB has a microphase-separated morphology. For simplicity, only a sphere symbol represents the mobile ions in the scheme, and X^+ denotes mobile cations existing in the polyelectrolyte membrane, which can include not only the cation of the IL, but also the cation in the sulfonate group of SSPB. This scheme compares the SSPB and its s-MMT nanocomposites with Nafion. (b) The molecular structure of the SSPB copolymer, (c) structure of the sulfonated silicate (s-MMT), and (d) molecular structure of the ILs used in this study. TEM images of (e) SSPB, (f) SSPB/s-MMT, and (g) Nafion. (h) Wide angle X-ray diffraction (WAXD) patterns of MMT, s-MMT, SSPB/MMT, and SSPB/s-MMT. The silicate content in the nanocomposites was 8 wt%.

Table 1 Characterization of SSPB, silicates, and SSPB/silicate nanocomposites[22,23]

	Block M_w[a] (kg mol^{-1})								
Copolymer	*t*BS	EP	S	EP	*t*BS	IEC[b] (meq. g^{-1})	SF[c] (mmol g^{-1})	d[d] (nm)	d_{001}[e] (nm)
SSPB	15.0	9.3	28.3	11.0	14.4	2.0	1.71	29.8	—
MMT						0.91	0	—	0.99
s-MMT						0.89	0.33	—	1.23
SSPB/MMT[f]							1.57	29.9	1.44
SSPB/s-MMT[f]							1.60	31.1	1.70

[a] The block molecular weight of the precursor polymer prior to the sulfonation. [b] Ion exchange capacity (mmol H^+ per 1 g polymer) determined by back titration. [c] The concentration of the sulfonic group determined by chemical composition. [d] Domain spacing between the microphase-separated ionic domains in the SSPB. [e] Layer spacing between the adjacent silicate layers. [f] The filler content was 8 wt%.

SSPB/MMT nanocomposites exhibited the characteristic layer spacing peak (d_{001}) of the layered silicates at smaller angles than the MMT and s-MMT fillers, respectively. This indicates that the SSPB/s-MMT and SSPB/MMT nanocomposites had an intercalated morphology in which the SSPB molecules were intercalated between the silicate layers so that the layer spacing between the adjacent silicate layers was expanded, as shown in Table 1. The SSPB/s-MMT peaked at a smaller angle than the SSPB/MMT, indicating that the s-MMT had a better dispersion state and a more developed intercalation than the MMT in the SSPB. In Fig. 1f, the TEM image of SSPB/s-MMT revealed that the SSPB/s-MMT achieved a well developed intercalated morphology, which was consistent with the results shown in Fig. 1h. It should be noted that silicate platelets were

homogeneously distributed in the SSPB matrix and placed over the several repeating domains of the SSPB nanostructured pentablock copolymer ionomer membrane.

SSPB/IL, SSPB/MMT/IL, and SSPB/s-MMT/IL IPMC actuators were prepared *via* an electroless plating method of platinum on both sides of each membrane, followed by impregnation with IL as the inner solvent in the IPMC.[3,20] The four imidazolium-based ionic liquids (C2, C4, C6, C8), introduced to each membrane, are shown in Fig. 1d (see the details of the chemical structures of the ILs in the ESI, Fig. S5†). The four imidazolium-based ILs have the same bis(trifluoromethylsulfonyl)imide (TFSI) anion, but a different imidazolium cation with different lengths of the linear hydrocarbon substituent on the N(1) position of the imidazolium cation. The number in the sample codes of ILs denotes the number of carbons in the hydrocarbon substituent; thus, the bulkiness of the IL increases with the increase in carbon number of the hydrocarbon substituent.

Fig. 2a shows small angle X-ray scattering (SAXS) patterns of the pristine SSPB and SSPB/IL membranes with C2, C4, C6, and C8 ILs. Each membrane had one Bragg reflection peak in the SAXS measurement. Bragg spacing (d) of the repeating domain unit, composed of alternating styrene-rich regions (ionic phase) and aliphatic EP-rich regions (non-ionic phase), in the SSPB matrix was calculated by Bragg's law ($d = 2\pi/q = n\lambda/2\sin\theta$). Impregnation of the SSPB block copolymer with ILs enlarged the domain spacing. The d values of neat SSPB, SSPB/C2, SSPB/C4, SSPB/C6, and SSPB/C8 were 29.8, 45.9, 45.2, 43.9, and 42.2 nm, respectively, which was on the line of hydrated SSPB with the domain spacing of 44.9 nm. In addition, incorporation of silicates (8 wt% of MMT and s-MMT) into the SSPB matrix further extended the spacing to a limited extent, especially with s-MMT (Fig. 2b and ESI, Fig. S6†). From the SAXS results, regardless of the presence of MMT and s-MMT, the spacing of the IL-incorporated SSPB membranes monotonously decreased with the increase in carbon number of the hydrocarbon substituent on the N(1) position of the imidazolium ring of IL. Fig. 2c shows the IL contents in the SSPB/IL, SSPB/MMT/IL, and SSPB/s-MMT/IL IPMCs (refer to ESI, Table S1† for the exact averaged values). The amount of IL uptake by the bare SSPB membrane monotonously increased with the increase in length of the linear alkyl substituent on the imidazolium cation of IL from 81 to 126 wt%. A cast Nafion membrane also showed the same tendency for IL uptake as that of SSPB, although the uptake levels of the Nafion membrane were lower than those of the SSPB membrane. The higher IL uptake level of the SSPB membrane was attributed not only to the larger concentration of sulfonic acid groups in the SSPB matrix, but also to the larger ionic channel size, compared with its Nafion counterpart.[2,21] The incorporation of MMT into the SSPB nanostructured block copolymer membrane augmented the uptake level, which was further increased through the introduction of s-MMT with sulfonic acid groups. This result is reasonable considering the hygroscopic nature of MMT and s-MMT. The sulfonic moieties on the s-MMT might induce an additional affinity between the SSPB nanocomposites and the imidazolium ILs, although the SSPB/s-MMT was less hygroscopic than the SSPB/MMT, as we reported in a previous paper.[21]

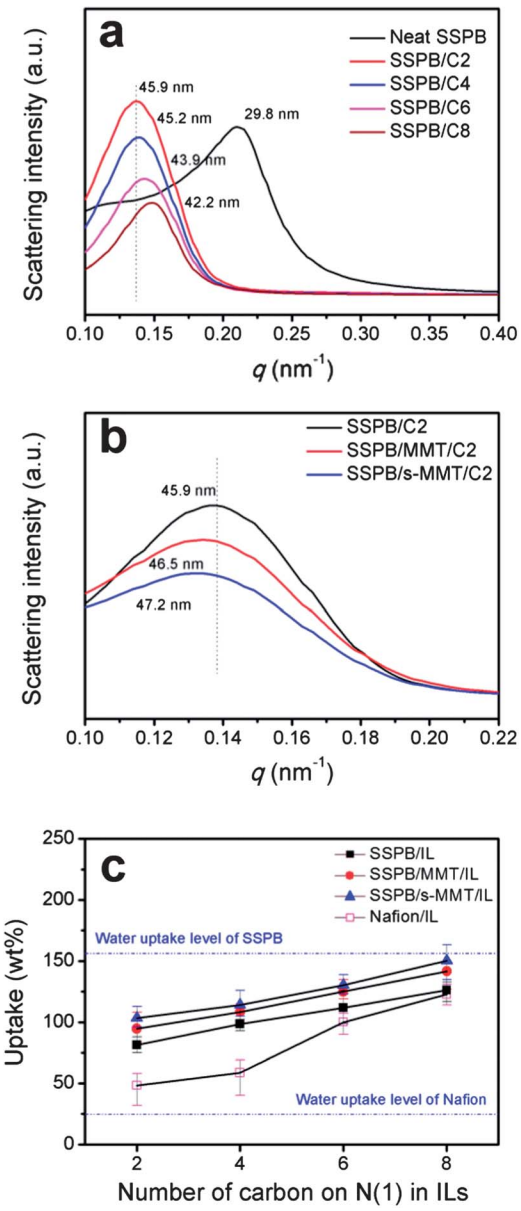

Fig. 2 SAXS profiles of (a) SSPB/IL membranes with a series of ILs (C2, C4, C6, and C8); (b) SSPB/IL, SSPB/MMT/IL, and SSPB/s-MMT/IL membranes with C2 IL; (c) IL uptake of SSPB/IL, SSPB/MMT/IL, SSPB/s-MMT/IL, and Nafion/IL. The value of uptake was obtained by the following equation: uptake (wt%) = $(W_i - W_n)/W_n \times 100$, where W_n and W_i are the weights of the neat and IL- or water-impregnated membranes, respectively. For the IL uptake experiment, SSPB membranes fully dehydrated in a vacuum oven were weighed to obtain W_n, then immersed in each mixture of IL–methanol (IL : methanol = 1 : 1, w/w) for 2 days at room temperature, and finally reweighed after the evaporation of methanol at 60 °C under vacuum to determine W_i. For the assessment of water uptake, the SSPB membranes that had been fully swollen in deionized water for 1 day at room temperature were wiped with a clean filter paper, and then reweighed immediately to determine W_i. The silicate content in the nanocomposites was 8 wt%.

From the results in Fig. 2a and c, as the carbon number of the substituent in the ILs increased, IL uptake increased, whereas the domain spacing of the SSPB-based membrane decreased. These results were attributed to the difference in the swelling selectivity of ILs towards the ionic domain of the SSPB. The swelling selectivity of the IL towards the ionic domain of the

SSPB decreases with the increase in the length of the hydrocarbon substituent on the imidazolium ring of the ILs, because the hydrophobicity of the IL increases with the increase in the length of the hydrocarbon substituent. More hydrophobic IL is more favorable to the non-ionic domain of SSPB. Less selective swelling produces weak segregation between ionic and non-ionic domains and causes smaller domain spacing.[25,26]

Fig. 3a shows the ion conductivities of the SSPB/IL, SSPB/MMT/IL, and SSPB/s-MMT/IL membranes. The ion conductivities of the SSPB/IL membranes decreased with the increase in carbon number on the N(1) position of the imidazolium ring of IL in the range of 2.21–0.29 $\times$ 10^{-4} S cm^{-1}, which were much smaller than those of the respective neat ILs (8.02–2.38 $\times$ 10^{-3} S cm^{-1}). The SSPB/MMT/IL and SSPB/s-MMT/IL nanocomposite membranes also revealed the same tendency as the SSPB/IL did. The decay in membrane ion conductivity observed from C2 to C8 was deeply related to the increase in the bulkiness and viscosity of IL, both of which make ion transport difficult in both cases of IL in the bulk state and inside the polymer ionomer.[4,14,27–29] The viscosities of C2, C4, C6, and C8 were 34,[30] 52,[30] 87.3,[31] and 119.3[31] cP, respectively. The SSPB/MMT/IL membranes had less ion conductivity than the SSPB/IL with the same ILs. However, interestingly, the SSPB/s-MMT/IL showed larger ion conductivities than the SSPB/IL, regardless of the IL used. The ionic conductivities of SSPB/s-MMT/C2, SSPB/s-MMT/C4, SSPB/s-MMT/C6, and SSPB/s-MMT/C8 were found to be 2.60, 2.15, 0.62, and 0.32 $\times$ 10^{-4} S cm^{-1}, respectively. The incorporation of s-MMT into the SSPB matrix resulted in a well dispersed intercalation morphology—silicate platelets placed over several repeating domains in the SSPB. Thus, the large ionic conductivities in the SSPB/s-MMT/IL membranes could be attributed to the presence of sulfonic groups on the highly intercalated s-MMT platelets that facilitate the transport of mobile ions between the adjacent wide ionic channels like an ionic bridge in the nanostructured SSPB membrane, as illustrated in Fig. 1a, due to the strong interaction between the sulfonic groups of SSPB and the sulfonic groups of s-MMT. This positive effect for ion conductivity seems to prevail against the decrease in sulfonic group density by the addition of s-MMT having a much higher density than the polymeric SSPB (the concentrations of sulfonic group for SSPB and SSPB/s-MMT were 1.71 mmol g^{-1} and 1.60 mmol g^{-1}, respectively). It should also be highlighted that the ionic conductivity values obtained from all the prepared SSPB-based membranes were larger than those of the Nafion counterpart, regardless of the ILs and silicate fillers used in this study.

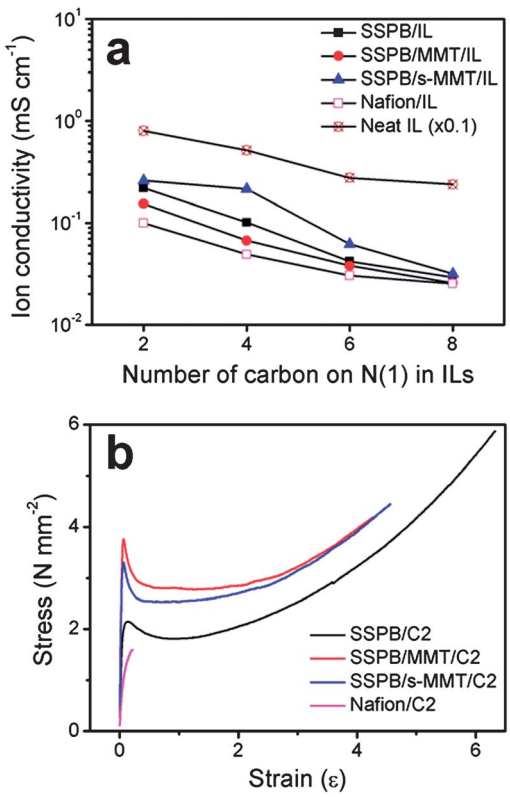

Fig. 3 (a) Ion conductivity of SSPB/IL, SSPB/MMT/IL, and SSPB/s-MMT/IL membranes with a series of ILs (C2, C4, C6, and C8). (b) Tensile stress–strain curves of the SSPB/IL, SSPB/MMT/IL, and SSPB/s-MMT/IL membranes incorporated with C2 IL. The silicate content in the nanocomposites was 8 wt%.

The mechanical properties of the SSPB/IL, SSPB/MMT/IL, and SSPB/s-MMT/IL membranes are shown in Table 2 and Fig. 3b. In spite of the enormous IL uptake, the SSPB/IL, SSPB/MMT/IL and SSPB/s-MMT/IL membranes maintained the ultimate elongation values of pristine SSPB of at least *ca.* 400%, while the Nafion/IL membranes had elongations at break of less than 45%. Generally, with more IL uptake in polymer membranes larger ion conductivities are exhibited.[3,14,32] An excessive IL uptake, however, decreases the mechanical strength of the membrane, and further IL uptake worsens even the bending strain.[6,12,21] Fascinatingly, the strong swelling selectivity of IL on the microphase-separated ionic domains of the SSPB pentablock copolymer could lead to excellent mechanical properties despite the large IL uptake level of up to 163 wt%. The selective swelling effect of IL prevents it from

Table 2 Mechanical properties of the SSPB/IL, SSPB/MMT/IL, and SSPB/s-MMT/IL membranes

Membrane	Ionic liquid	Modulus (MPa)	Elongation at break (%)
SSPB/IL	C2	40.2	633
	C4	4.5	563
	C6	1.9	604
	C8	0.5	548
SSPB/MMT/IL[a]	C2	66.5	429
	C4	6.1	501
	C6	3.8	564
	C8	0.5	535
SSPB/s-MMT/IL[a]	C2	89.0	457
	C4	10.2	398
	C6	4.1	393
	C8	0.7	532
Nafion/IL	C2	14.2	22
	C4	7.2	40
	C6	4.2	44
	C8	2.3	17

[a] The silicate content in the nanocomposites was fixed at 8 wt%.

easily plasticizing the non-ionic phases responsible for the mechanical strength. The incorporation of MMT and s-MMT increased the tensile modulus of SSPB during the initial stage of tensile deformation. The SSPB/s-MMT nanocomposite had a larger tensile modulus than the SSPB/MMT because of its better intercalation state. The tensile moduli of the SSPB-based membranes considerably decreased with increasing carbon number on the N(1) position of the imidazolium ring of IL. Considering the IL uptake and the SAXS results, the smaller moduli of the membranes incorporating ILs with longer alkyl substituents could be attributed not only to a higher IL uptake level, but also to less selective swelling of the IL towards the ionic domains in the SSPB matrix.

The electromechanical responses of the IPMC actuators based on the SSPB/IL, SSPB/MMT/IL, and SSPB/s-MMT/IL membranes were evaluated through measuring the horizontal displacement at the tip of the cantilever (with a free length of 20 mm) under 2 V dc during the 10 min bending actuation. In Fig. 4a, the bending displacement of the SSPB/IL IPMCs loaded with different ILs followed the order of C8 ≈ C6 > C4 > C2. The bending displacements of the SSPB/MMT/IL and SSPB/s-MMT/IL IPMCs revealed the same tendency as that of SSPB/IL IPMC (ESI, Fig. S7†). In addition, all the examined IPMCs did not show any evidence of back relaxation during the actuation period of 10 min. Generally, a higher conductivity of a polymer membrane leads to a larger bending deformation in the IPMC.[16,17] However, the actuation performance order of the SSPB-based IPMCs with the four imidazolium ILs (C8 ≈ C6 > C4 > C2) mismatched the membrane ion conductivity result, which was in the order of C2 > C4 > C6 > C8.

The bending tip displacements of the SSPB/C6, SSPB/MMT/C6, and SSPB/s-MMT/C6 IPMCs incorporating C6 IL are presented in Fig. 4b. Fig. 4c shows a representative time-dependent bending motion of the SSPB/s-MMT/C6 IPMC. The bending actuation of the SSPB-based IPMCs was much larger and faster than that of the Nafion-based IPMCs. The displacements and the response rates followed the order of SSPB/s-MMT/C6 > SSPB/C6 > SSPB/MMT/C6 IPMCs, which was approximately the same as that of the membrane ion conductivity results.

To the best of our knowledge, the maximum bending displacement of the SSPB/s-MMT/C6 IPMC, which measured an average of 10.2 mm under 2 V dc within the given 10 min, was superior to those of top-ranked IL-incorporated ionic polyelectrolytes, such as radiation-grafted fluoropolymer/IL,[4] semi-IPN/IL,[33–35] ABA-triblock copolymer (PS-*b*-PMMA-*b*-PS)-based ionic gel actuators,[36] and bucky-gel actuators.[37–40] Moreover, despite the use of bulky IL to give stable air-operation ability to the IPMC, the bending performance of the SSPB/s-MMT/C6 IPMC in terms of displacement and response rate was substantially superior to that of the SSPB/s-MMT/water IPMC (SSPB/s-MMT/water IPMC: 4.6 mm after 2 min actuation at 2 V dc with the identical free lengths of specimen).[21]

The largest and fastest bending performance of SSPB/s-MMT was attributed not only to the large SSPB's ion domains but also to the strong interactions between the mobile ions and the sulfonic groups on the s-MMT. Although the ionic liquid molecules are much bigger than water molecules, the ionic domains of SSPB, which are much bigger than that of IL, facilitated the mass transport of the bulky mobile ions. The strong interactions between the mobile ions and the sulfonic groups on the s-MMT promote the ion transport between the ionic domains in SSPB, resulting in the improvement of ion conductivity. That is, sulfonated silicates act as ionic bridges

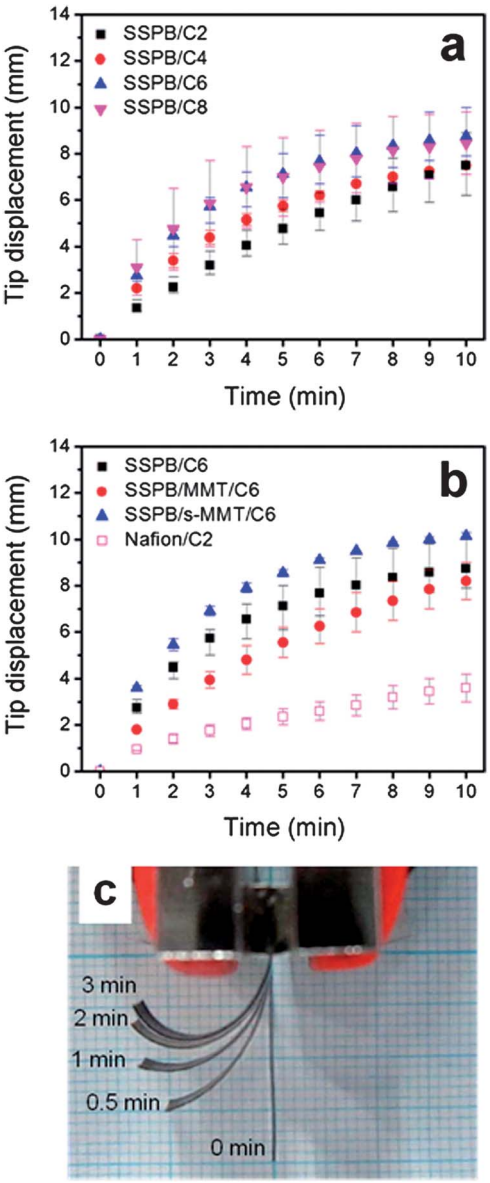

Fig. 4 Tip displacement *vs.* time curves of IPMCs based on SSPB/IL, SSPB/MMT/IL and SSPB/s-MMT/IL membranes under an applied voltage of 2 V dc: (a) SSPB/IL IPMCs with a series of ILs (C2, C4, C6, and C8); (b) SSPB/IL, SSPB/MMT/IL, and SSPB/s-MMT/IL IPMCs incorporating with C6 IL. The nanocomposite membranes as polymer electrolytes of the IPMCs had a silicate content of 8 wt%. IPMC strips with dimensions of 23 mm in length and 3 mm in width were vertically fixed to 3 mm length by a platinum grip, and thus the actual free length of the strips was 20 mm. The tip displacement was obtained by measuring the horizontal displacement of the IPMC strips at the tip 20 mm away from the grip. For rational comparison, the overall thickness of the IPMCs was controlled to 0.23 ± 0.02 mm. All the IPMC actuators had an electrode thicknesses of 5 μm and the corresponding surface resistances of 4–9 Ω. (c) Visualized time-dependent bending motion of the SSPB/s-MMT/C6 IPMC taken under an applied potential of 5 V dc.

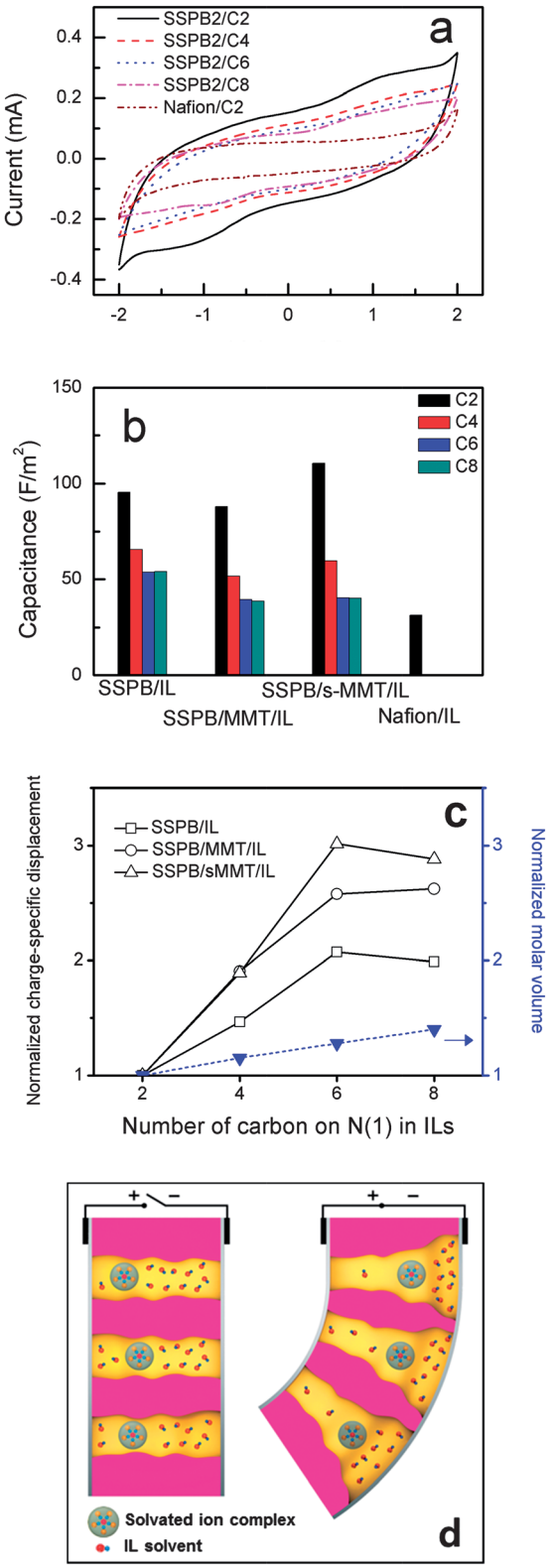

Fig. 5 (a) Cyclic voltammograms of IPMCs based on SSPB/IL membranes. (b) Capacitances of SSPB/IL, SSPB/MMT/IL, and SSPB/s-MMT/IL IPMC actuators assessed through the corresponding CV traces. The CV measurement *via* a two-electrode system was performed by connecting the counter- and reference-electrode leads to one side of the IPMC and by connecting the working electrode lead to the other side, with a potential range of −2 to 2 V and a scan rate of 50 mV s^{-1}. (c) Normalized charge-specific displacements for SSPB/IL, SSPB/MMT/IL, and SSPB/s-MMT/IL IPMC actuators and normalized molar volumes of imidazolium ILs (C2, C4, C6, and C8). The charge-specific displacement, which is the maximum tip displacement (attained within 10 min under 2 V dc) divided by the capacitance, was normalized by that of each C2-impregnated IPMC with the identical framework. The molar volumes of ILs, which were calculated using the corresponding densities, were also normalized by that of C2. The nanocomposite membranes as polymer electrolytes of the IPMCs had a silicate content of 8 wt%. (d) An illustration of the pumping effect in the nanostructured polymer ionomers with big ion channels. The mobile ions, solvated with inner solvent, pump loosely bound solvent molecules as a piston in the ionic channels under an applied voltage when the sizes of the solvated ion complex and the channel match with each other. The ion pumping effect makes the nanostructured polymer ionomers have a large bending displacement and fast response rate.

accelerating the mass transport of mobile ions between the ionic domains.

Nonetheless, the reverse order of the actuation performance of SSPB-based IPMCs with the four imidazolium ILs (C8 ≈ C6 > C4 > C2) and the membrane conductivity (C2 > C4 > C6 > C8) has not yet been explained. To further understand the phenomenon, the capacitance—another critical factor determining the bending deformation—was considered.

The cyclic voltammetry (CV) profiles of SSPB/IL IPMCs with C2–C8 and Nafion/C2 IPMC are shown in Fig. 5a (see ESI, Fig. S8† for the CV results of SSPB/MMT/IL and SSPB/s-MMT/IL IPMCs). The capacitances with respect to the area of electrode determined from the CV data are summarized in Fig. 5b. No faradic current was observed in the CV profiles within a potential range of −2 to 2 V with a scan rate of 50 mV s^{-1}. This observation indicates that there was no electrolysis of the imidazolium ILs in the potential range. ILs with shorter hydrocarbon substituents on the N(1) position of the imidazolium cation gave larger capacitances to the SSPB/IL IPMCs because the bulkiness of imidazolium cation sterically hinders charging at the interface between the membrane and electrode.[27] From this consideration, it makes sense that the SSPB-based IPMCs possessing big ionic channels have capacitances larger than the Nafion benchmark because of a wide interface between the platinum electrode and the ionic domain of SSPB. Meanwhile, the SSPB/IL IPMCs revealed larger capacitances than both the SSPB/MMT/IL and SSPB/s-MMT/IL IPMCs. This observation might be due to the same steric hindrance of the silicate fillers located in the interface between the electrode and the ionic domain of SSPB.

The normalized charge-specific displacements for SSPB/IL, SSPB/MMT/IL, and SSPB/s-MMT/IL IPMC actuators are exhibited in Fig. 5c. The charge-specific displacement representing the contribution of a mobile ion to the bending displacement was normalized based on the values of the C2-incorporated sample of respective SSPB, SSPB/MMT, and SSPB/s-MMT frameworks. The normalized charge-specific displacement increased as the bulkiness of the IL increased and the saturation was observed at C6. In general, bulkier ions have larger contributions from mobile ions to the bending displacement because of their larger volume per unit ion. However, the normalized charge-specific displacement of SSPB-based IPMCs incorporating bulky IL must not be attributed merely to the bulkiness of mobile imidazolium cations. The SSPB/C6, SSPB/MMT/C6, and SSPB/s-MMT/C6 IPMCs had the normalized

charge-specific displacements of 2.1, 2.6, and 3.0, respectively, which were much larger than the normalized molar volumes of C6 of 1.3. The molar volume of each IL was calculated using IL densities (C2: 1.542, C4: 1.433, C6: 1.378, and C8: 1.337).[41] The behavior could be interpreted by an ion-pumping model, proposed by Onishi *et al.*[42] The mobile ions, solvated with inner solvent, pump loosely bound solvent molecules as a piston in the ionic channels under an applied voltage when the sizes of the solvated ion complex and the channel match well with each other. In the air-working SSPB-based IPMC actuators, in addition to the dissociated mobile imidazolium cations of IL, the abundant associated ion pairs of IL, which are not a source of current and play as an inner solvent, were migrated by ion pumping effect as illustrated in Fig. 5d.[27] This pumping effect led to larger bending displacements of IPMCs per unit charge. The pumping effect, depending on the viscosity of IL, indicated that bulky ILs presented stronger pumping effects than small ILs. Despite a relatively big mismatch of the sizes of the mobile ions (below 2 nm in length for all ionic species including two ions from IL and a counter ion from SSPB) and the ionic channels (the diameter of approximately 20 nm), the pumping effect, obviously observed in our SSPB/IL system, was probably due to a loose size-matching between the big ion channel of SSPB and the highly viscous imidazolium ILs compared with water.

With the same IL, the normalized charge-specific displacements followed the order of SSPB/s-MMT/IL > SSPB/MMT/IL > SSPB/IL IPMCs. The largest normalized charge-specific displacement of SSPB/s-MMT was also attributed to the strong ion pumping effect of SSPB/s-MMT/IL IPMC caused by the strong interactions between the solvated mobile ions and the sulfonic acid groups on the s-MMT.

To the best of our knowledge, this is the first paper that reports the nanostructured ionomer/functionalized filler nanocomposite membranes incorporating IL presenting much larger actuation displacement and much faster response than not only the pristine polyelectrolyte membrane and the Nafion membrane incorporating IL but also their hydrated ones. Moreover, bulky IL-incorporated membranes generated much larger and faster bending responses than small IL-incorporated ones. This observation was attributed to the strong pumping effect of bulky IL in the ionic domains bigger than the IL.

Experimental

Materials

Poly((*t*-butyl-styrene)-*b*-(ethylene-*r*-propylene)-*b*-(styrene-*r*-styrene sulfonate)-*b*-(ethylene-*r*-propylene)-*b*-(*t*-butyl-styrene)) (*t*BS-EP-SS-EP-*t*BS; SSPB) pentablock copolymer ionomer with 10 wt% dispersion in a mixed solvent of heptane and cyclohexane (MD-9200, Kraton Polymers) was used. The SSPB had an ion exchange capacity (IEC) value of 2.0 meq. g^{-1} (2.0 mmol H^+ per 1 g polymer). The sodium montmorillonite (MMT) (Cloisite Na^+, cation exchange capacity of 0.91 meq. per 1 g silicate) was donated by Southern Clay Products. Four imidazolium ionic liquids (ILs) were custom-made with a high purity of >99.9% by C-TRI in Korea: 1-ethyl-3-methylimidazolium bis(trifluoromethylsulfonyl) imide (C2), 1-butyl-3-methylimidazolium bis(trifluoromethylsulfonyl)imide (C4), 1-hexyl-3-methylimidazolium bis(trifluoromethylsulfonyl)imide (C6), 1-octyl-3-methylimidazolium bis(trifluoromethylsulfonyl)imide (C8). As the ionic polymer electrolyte reference, a Nafion dispersion (DE-2021, 0.95 IEC, DuPont) was used. 3-Mercaptopropyltrimethoxy silane (3-MPTMS) and the other reagents were research grade and were used without further purification.

Functionalization of silicates

The sulfonated MMT (s-MMT) was synthesized from MMT *via* a series of silylation/oxidation reactions using an organosilane (3-MPTMS) to give ionic moieties and better dispersion in the polymer electrolyte matrices.[21] The resulting s-MMT had a sulfonic group density of 0.33 mmol g^{-1} (ESI, Fig. S1–S4†).

Preparation of nanostructured block copolymer ionomer/silicate/ionic liquid membranes and IPMCs

A predetermined amount of MMT or s-MMT as a filler was added to the SSPB copolymer dispersion and stirred for at least 3 days and then dispersed under sonication. The filler content was fixed to 8 wt%. After that, the clear dispersion was cast onto a glass plate, followed by slow evaporation of solvent through covering the cast with a perforated lid at room temperature. The thickness of the membrane was controlled using a bar coater (Comate 3000VH, KIPAE Engineering and Technology) (ESI, Table S2† for description of the membrane-thickness control and the resulting thickness values). The obtained membranes were thermally annealed at 120 °C for 2 h to enhance their mechanical strength and ionic transport,[21] and then protonated and cleaned through boiling in 2 N HCl and deionized water for 30 min each. The IPMCs were constructed by coating both membrane surfaces with platinum electrodes *via* electroless plating (refer to ESI for the detailed procedure†). The surface resistance of each electrode was below 10 Ω. For completion of the IPMCs based on the nanostructured block ionomer/silicate/ionic liquid membranes, the IL-free IPMCs were soaked in each mixture of methanol and one of C2, C4, C6, or C8 ILs (methanol : IL = 1 : 1, w/w) for 2 days at room temperature, followed by the evaporation of methanol at 60 °C under vacuum.

Characterization

The morphology of the nanocomposites was observed *via* a scanning transmission electron microscope (STEM, CM-30, Philips) with an energy-dispersive X-ray spectrometer (EDS, DX-4, EDAX). The ultrathin sections of the samples for STEM examination were sliced using a cryomicrotome (Ultracut UCT, LEICA) at −120 °C. Each specimen for STEM analysis was stained with a 0.5% ruthenium tetroxide (RuO_4) aqueous solution. The intercalation states of MMT and s-MMT in the nanocomposites were measured using a wide angle X-ray diffraction (WAXD, D/Max-2200, Rigaku Denki, Japan) under 40 kV and 30 mA of Cu Kα radiation with a characteristic wavelength of 0.154 nm and a scanning rate of 4° min^{-1}. Proton conductivities of the SSPB-based membranes were measured with a potentiostat/galvanostat/electrochemical impedance spectroscopy (EIS)

instrument (VMP3, BioLogic Science Instruments, France), combined with a custom-made two-probe cell. The tensile test was carried out using a universal test machine (H5KT, Tinius Olsen, USA) with a cross header speed of 20 mm min^{-1}. The microphase-separated structures of the membranes were analyzed using a synchrotron small angle X-ray scattering (SAXS) of the Pohang Accelerator Laboratory (PAL, Pohang, Korea). For the electromechanical test, bipolar voltages on the IPMC actuators were applied using the EIS instrument. The displacement measurement was performed using a CCD camera connected to a computer with a data acquisition (DAQ) system (SCB-68, National Instrument, USA). Capacitances of the IPMCs were measured using the EIS instrument with a voltage range of −2 to 2 V and a scan rate of 50 mV s^{-1} in the two-electrode system. All samples were completely dried in a vacuum oven at 60 °C prior to measurement to minimize any experimental errors produced by moisture.

Conclusions

The SSPB nanostructured pentablock copolymer ionomer/sulfonated silicate nanocomposite membranes incorporating bulky imidazolium ionic liquids revealed much larger bending displacements and faster actuation rates than the SSPB/IL and Nafion/IL membranes, operating in air without the conventional IPMC drawbacks of back relaxation and sacrifice of mechanical strength. Moreover, the air-working IL-incorporated SSPB/s-MMT nanocomposite IPMC revealed not only a longer service life, but also a larger bending strain than the hydrated SSPB/s-MMT IPMC. The highly distinctive air-working actuation performance, far beyond that of the Nafion counterpart, of the SSPB/s-MMT/IL IPMC should be attributed to the attainment of the high ion conductivity through the enormous IL uptake together with the preservation of the inherent mechanical property. The effective mass transport of mobile ions for the bending motion is attributed to the well-defined microphase-separated big-size ionic domain morphology of the SSPB copolymer on the scale of several tens of nanometers and to the bridging effect of sulfonic groups on the s-MMT. Interestingly, as the bulkiness of the IL increased, the ion conductivity decreased, whereas the normalized bending strain and charge-specific displacement of the SSPB/s-MMT/IL IPMC increased. This was caused by the bulky mobile ions of IL, producing strong pumping effects in the nanostructured SSPB ionomer-based membranes containing ionic domains bigger than the mobile ions and solvent. We demonstrated a useful protocol to design a new generation of nanostructured block copolymer ionomer nanocomposite membranes incorporating ion conduction-activating fillers for the air-working IPMC transducers. It can readily be extended to other applications with structural similarity, including fuel cells, capacitors, and a variety of other electronic devices.

Acknowledgements

This work was supported by the Fundamental R&D Program for Core Technology of Materials funded by the Ministry of Knowledge Economy, Republic of Korea and partially by the Korea Institute of Science and Technology. SAXS experiments were performed in Pohang Light Source. We would also like to give special thanks to Dr Jang Yeol Lee for valuable and sincere discussions about experimental methods and data and to Dr Saeed Doroudiani for the advice in the editing of the manuscript.

Notes and references

1 M. Shahinpoor, Y. Bar-Cohen and J. O. Simpson, *Smart Mater. Struct.*, 1998, **7**, R15.
2 M. Shahinpoor and K. J. Kim, *Smart Mater. Struct.*, 2001, **10**, 819.
3 A. J. Duncan, B. J. Akle, T. E. Long and D. J. Leo, *Smart Mater. Struct.*, 2009, **18**, 104005.
4 J. Y. Lee, H. S. Wang, B. R. Yoon, M. J. Han and J. Y. Jho, *Macromol. Rapid Commun.*, 2010, **31**, 1897.
5 M. Shahinpoor, K. J. Kim and D. J. Leo, *Polym. Compos.*, 2003, **24**, 24.
6 J.-W. Lee, J.-H. Kim, N. S. Goo, J. Y. Lee and Y.-T. Yoo, *J. Bionic Eng.*, 2010, **7**, 19.
7 M. Luqman, J.-W. Lee, K.-K. Moon and Y.-T. Yoo, *J. Ind. Eng. Chem.*, 2011, **17**, 49.
8 B. J. Akle, D. J. Leo, M. A. Hickner and J. E. McGrath, *J. Mater. Sci.*, 2005, **40**, 3715.
9 A. K. Phillips and R. B. Moore, *Polymer*, 2005, **46**, 7788.
10 M. J. Han, J. H. Park, J. Y. Lee and J. Y. Jho, *Macromol. Rapid Commun.*, 2006, **27**, 219.
11 J. Lu, S.-G. Kim, S. Lee and I.-K. Oh, *Adv. Funct. Mater.*, 2008, **18**, 1290.
12 J.-W. Lee, K. N. Vinh, S.-Y. Park and Y.-T. Yoo, *J. Korean Phys. Soc.*, 2006, **48**, 1594.
13 M. D. Bennett and D. J. Leo, *Sens. Actuators, A*, 2004, **115**, 79.
14 B. J. Akle, M. D. Bennett and D. J. Leo, *Sens. Actuators, A*, 2006, **126**, 173.
15 H. M. Jeong, S. M. Woo, S. Lee, G.-C. Cha and M. S. Mun, *J. Appl. Polym. Sci.*, 2005, **99**, 1732.
16 R. Tiwari and E. Garcia, *Smart Mater. Struct.*, 2011, **20**, 083001.
17 A. J. Duncan, D. J. Leo and T. E. Long, *Macromolecules*, 2008, **41**, 7765.
18 X. L. Wang, I. K. Oh, J. Lu, J. Ju and S. W. Lee, *Mater. Lett.*, 2007, **61**, 5117.
19 P. H. Vargantwar, R. Shankar, A. S. Krishnan, T. K. Ghosh and R. J. Spontak, *Soft Matter*, 2011, **7**, 1651.
20 P. H. Vargantwar, K. E. Roskov, T. K. Ghosh and R. J. Spontak, *Macromol. Rapid Commun.*, 2012, **33**, 61.
21 J.-W. Lee, S. M. Hong, J. Kim and C. M. Koo, *Sens. Actuators, B*, 2012, **162**, 369.
22 G. M. Geise, B. D. Freeman and D. R. Paul, *Proceedings of the 67th Annual Technical Conference & Exhibition – ANTEC 2009*, Chicago, 2009.
23 G. M. Geise, B. D. Freeman and D. R. Paul, *Polymer*, 2010, **51**, 5815.
24 C. H. Rhee, H. K. Kim, H. Chang and J. S. Lee, *Chem. Mater.*, 2005, **17**, 1691.

25 T. P. Lodge, K. J. Hanley, B. Pudil and V. Alahapperuma, *Macromolecules*, 2003, **36**, 816.
26 S. Y. Kim, S. Kim and M. J. Park, *Nat. Commun.*, 2010, **1**, 88.
27 J.-W. Lee and Y.-T. Yoo, *Sens. Actuators, B*, 2009, **137**, 539.
28 R. Hagiwara, K. Matsumoto, Y. Nakamori, T. Tsuda, Y. Ito, H. Matsumoto and K. Momota, *J. Electrochem. Soc.*, 2003, **150**, D195.
29 R. Hagiwara and Y. Ito, *J. Fluorine Chem.*, 2000, **105**, 221.
30 P. Bonhôte, A.-P. Dias, N. Papageorgiou, K. Kalyanasundaram and M. Grätzel, *Inorg. Chem.*, 1996, **35**, 1168.
31 S. Zhang, N. Sun, X. He, X. Lu and X. Zhang, *J. Phys. Chem. Ref. Data*, 2006, **35**, 1475.
32 M. L. Hoarfrost and R. A. Segalman, *Macromolecules*, 2011, **44**, 5281.
33 F. Vidal, C. Plesse, D. Teyssié and C. Chevrot, *Synth. Met.*, 2004, **142**, 287.
34 F. Vidal, C. Plesse, G. Palaprat, A. Kheddar, J. Citerin, D. Teyssié and C. Chevrot, *Synth. Met.*, 2006, **156**, 1299.
35 F. Vidal, C. Plesse, G. Palaprat, J. Juger, J. Citerin, A. Kheddar, C. Chevrot and D. Teyssié, *Adv. Sci. Technol.*, 2008, **61**, 8.
36 S. Imaizumi, H. Kokubo and M. Watanabe, *Macromolecules*, 2012, **45**, 401.
37 T. Fukushima, K. Asaka, A. Kosaka and T. Aida, *Angew. Chem., Int. Ed.*, 2005, **44**, 2410.
38 T. Sugino, K. Kiyohara, I. Takeuchi, K. Mukai and K. Asaka, *Sens. Actuators, B*, 2009, **141**, 179.
39 N. Terasawa, I. Takeuchi and H. Matsumoto, *Sens. Actuators, B*, 2009, **139**, 624.
40 I. Takeuchi, K. Asaka, K. Kiyohara, T. Sugino, N. Terasawa, K. Mukai, T. Fukushima and T. Aida, *Electrochim. Acta*, 2009, **54**, 1762.
41 C. A. Ohlin, P. J. Dyson and G. Laurenczy, *Chem. Commun.*, 2004, 1070.
42 K. Onishi, S. Sewa, K. Asaka, N. Fujiwara and K. Oguro, *Electrochim. Acta*, 2001, **46**, 1233.